WPMST2-PR(18) 20885

F Causa et al.

Runaway Electron Imaging Spectrometry (REIS) system

Preprint of Paper to be submitted for publication in
Review of Scientific Instruments

This work has been carried out within the framework of the EUROfusion Consortium and has received funding from the Euratom research and training programme 2014-2018 under grant agreement No 633053. The views and opinions expressed herein do not necessarily reflect those of the European Commission.

Runaway Electron Imaging Spectrometry (REIS) system

F. Causa,[1, a)] M. Gospodarczyk,[2] P. Buratti,[3] D. Carnevale,[2] R. De Angelis,[3] B. Esposito,[3] A. Grosso,[3] G. Maddaluno,[3] J. R. Martin-Solis,[4] V. Piergotti,[3] Z. Popovic,[4] G. Rocchi,[3] A. Sibio,[3] C. Sozzi,[1] B. Tilia,[3] M. Valisa,[5] and the FTU Team[6]

[1)] *Istituto di Fisica del Plasma, Consiglio Nazionale delle Ricerche, via R. Cozzi, 53, 20125 Milano, Italy*

[2)] *Dip. di Ing. Civile e Ing. Informatica, Università di Roma, Tor Vergata, 00133 Roma, Italy*

[3)] *ENEA, Dipartimento FSN, C. R. Frascati, Via E. Fermi 45, 00044 Frascati (Roma), Italy*

[4)] *Universidad Carlos III de Madrid, Avda. Universidad 30, Leganes, 28911-Madrid, Spain*

[5)] *Istituto Gas Ionizzati, Consiglio Nazionale delle Ricerche, Consorzio RFX, Corso Stati Uniti, 4 35127 Padova, Italy*

[6)] *see the appendix of G. Pucella et al, Proceedings of the 26th IAEA Fusion Energy Conf. Kyoto, Japan, 2016, OV/P-4*

(Dated: 2 July 2018)

A portable Runaway Electron Imaging and Spectroscopy System (REIS) was developed in ENEA-Frascati to measure synchrotron radiation spectra from in-flight runaway electrons in tokamaks. The REIS is a wide-angle optical system with two lines of sight to collect simultaneously visible and infrared emission spectra using an incoherent bundle of fibers, in a spectral range that spans from 300 nm to 2500 nm, and visible images of the runaway electron beam using a CCD color micro camera at a rate of 25 frames per second. The REIS system is supervised and managed using a dedicated LabVIEW program, to acquire data simultaneously from three spectrometers every 20 ms (configurable down to 10 ms). An overview of the REIS architecture and acquisition system, and resulting experimental data obtained in FTU are presented and discussed in this paper.

PACS numbers: Valid PACS appear here
Keywords: REIS, runaway electron, diagnostic, FTU, synchrotron radiation

I. INTRODUCTION

Runaway Electrons (REs) are beams of electrons accelerated to velocities close to the speed of light. They represent a major concern in tokamaks because when they are lost to the first wall, significant local energy deposition, local melting and damage of plasma-facing components may occur. Key to the successful operation of tokamaks, and in particular of ITER and future energy-generation reactors of the DEMO type is the ability to control REs to mitigate their impact on machine operation. Such issues can be studied in detail in dedicated programs in smaller experiments that permit the realization of relevant scenarios involving significant fractions of REs. In this context, the recent integration of different diagnostics and new software tools within the FTU real-time RE control system ([1],[2]) is contributing to the characterization of RE dynamics and to the study of effective mitigation strategies[3]. A specific activity was focused on the design, development and construction of a new diagnostic, referred to as REIS (RE Imaging and Spectroscopy system), to detect and study in-flight REs. Synchrotron radiation measurements using imaging and spectral analysis provide a tool to detect the presence of REs when they are still confined within the plasma, and to deduce their energy from measured spectra and pitch angle. The REIS prototype was designed to be portable to medium size tokamaks such as AUG and TCV (installation procedures and results obtained in these machines will be presented elsewhere). The system permits the simultaneous detection of VIS/NIR spectra of synchrotron radiation and images from in-flight REs. The REIS data provide indirect information on the RE energy distribution function in the various phases of a discharge, particularly during RE plateaus following disruption events in which a large part of the plasma current is carried by relativistic electron beams.

Synchrotron radiation is emitted by charged particles moving at relativistic speeds in magnetic fields. When the electron speed approaches that of light the emission pattern is directed in a narrow beam in the direction of motion of the electron. The emission power depends on electron energy, pitch angle and magnetic field intensity, thus making it possible to estimate from calibrated spectra and images, the most important RE parameters, namely, pitch angle θ, beam radius, maximum energy and current.

The brightness of the measured synchrotron radiation

[a)] Electronic mail: causa@ifp.cnr.it

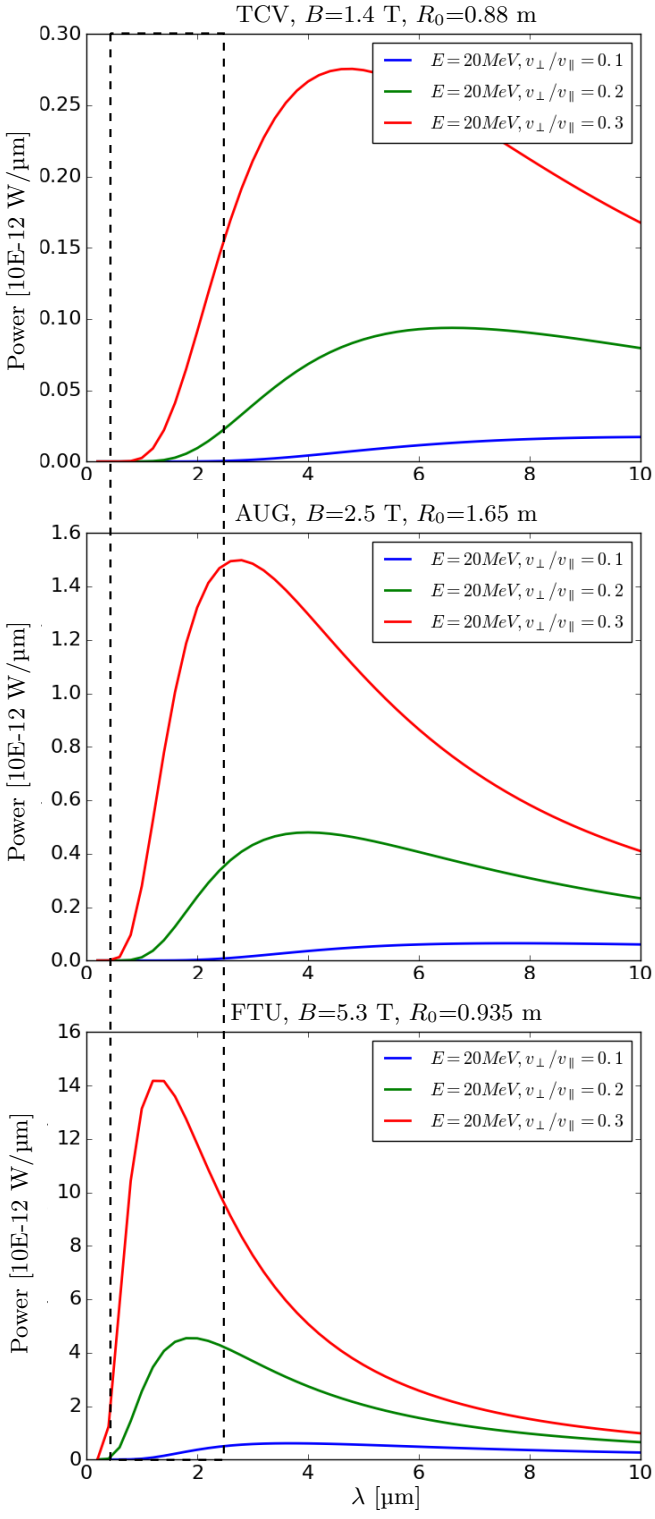

FIG. 1. Synchrotron emission spectra calculated using equation (1) for TCV, AUG and FTU at different energies and different pitch angle parameters $\frac{v_\parallel}{v_\perp} = \tan(\theta)$. Dashed lines show the actual REIS spectral range

can be expressed, as done in[4,5], as

$$B_r(\lambda,\theta,\gamma) = P(\lambda,\theta,\gamma)\frac{2R}{\pi\theta}n_{RE} \quad (1)$$

where n_{RE} is the density of the observed REs, R is the torus major radius, θ the pitch angle and $P(\lambda,\theta,\gamma)$ is the synchrotron power spectrum emitted by a single runaway electron. The synchrotron power spectrum, in cylindrical approximation, can be expressed as[5],

$$P_{cyl}(\lambda,\theta,\gamma) = \frac{ce^2}{\sqrt{3}\epsilon_0\lambda^3\gamma^2}\int_{\lambda_c/\lambda}^{\inf} K_{5/3}(l)dl \quad (2)$$

where e is the electron charge, c is the speed of light, ϵ_0 is the vacuum permittivity, $K_v(x)$ is the modified Bessel function of second kind, γ is the relativistic factor, λ is the the wavelength, and λ_c is a critical wavelength expressed by

$$\lambda_c = \frac{4\pi}{3}\frac{cm_e\gamma_{||}}{eB\gamma^2} \quad (3)$$

with m_e the electron rest mass and $\gamma_{||} = (1 - v_{||}^2/c^2)^{-0.5}$ the relativistic factor corresponding to the motion parallel to the magnetic field B. The cylindrical approximation is valid only for small pitch angles and does not take into account the effects of magnetic field line curvature and curvature drift, typical of a tokamak geometry. In tokamaks, such effects have to be taken into account,[5], for a correct description of the synchrotron emission spectrum.

Synchrotron radiation spectra in tokamak devices are typically peaked in the infrared part of the spectrum. Figure 1 shows the theoretical curves obtained using equation (1) for mono-energetic electrons in three tokamak devices with increasing magnetic fields (from the top: TCV, AUG and FTU). The spectra presented in Figure 1 demonstrate the importance of detecting synchrotron spectra in the infrared to capture a significant part of the curve to improve data interpretation capability. The REIS diagnostic was developed specifically with this purpose in mind. The REIS provides at present spectral measurements in the visible and near infrared. Details of the REIS system assembly and examples of experimental data collected in FTU are presented and discussed in the following Sections.

II. REIS DIAGNOSTIC

A. Detection system

A schematic of the REIS diagnostic is presented in Figure 2: it is a wide-angle optical system with two lines of sight (LoS), Figure 3(a), that are essentially coincident considering the vessel dimensions. A wide-angle objective lens (f = 3 mm) coupled to a visible CCD camera (Toshiba) is placed at the receiving end of LoS1 to collect the visible video images of the vessel cross-section

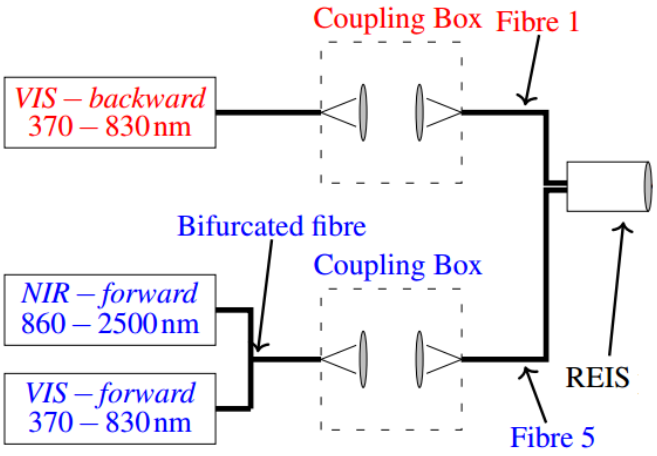

FIG. 2. REIS diagnostic schematic layout: the probe head comprises a wide-angle lens coupled to a CCD camera for the acquisition of visible images of the vessel poloidal cross-section (LoS1), and a second wide-angle lens coupled, through a set of lenses, to visible and infrared spectrometers for the acquisition of synchrotron spectra (LoS2).

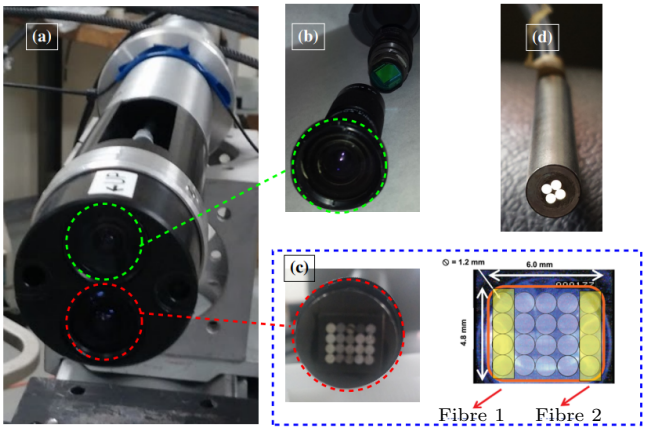

FIG. 3. REIS main optical components: (a) picture of the optical head; (b) picture of the objective lens, CCD camera and housing of LoS 1 (imaging); (c) picture and schematic of LoS2, showing the 5x4 incoherent fiber bundle overlapped with an image of the FTU vessel cross-section taken with the same CCD camera, the highlighted sections show the image sections used to capture the signal for the spectral analysis; (d) picture of one of the straight bare 4-fibre bundle outputs.

comprising both in-coming (forward view) and out-going (backward view) REs directions of flight, corresponding to the two poloidal sections of the vessel. The CCD camera is characterized by a 5.5 mm x 6 mm active area. LoS2, Figure 3(b), is equipped with a wide-angle camera lens with the same characteristics of the one coupled to the CCD camera. The objective lens is coupled to an incoherent, 20-fiber bundle, arranged as an array of 5 columns of 4 low-OH optical fibers. A schematic of the incoherent bundle of 20 fibres superimposed to the cross section image of the FTU vessel is presented in Figure 3(c). The fiber bundle was designed to permit five straight bare outputs of four-fibre bundles, as shown in Figure 3(d). Any of the five individual outputs can be connected to a spectrometer to detect and measure the optical spectrum of the collected radiation. However, considering the geometry of the diagnostic and the vessel cross-section intercepted by the diagnostic, the fiber outputs of interest correspond to the first and last columns, Figure 3(c). These are then connected to the spectrometers using a set of coupling lenses, Figure 2, with the dual purpose of mixing the optical signal collected via the individual fibers in each column, and of providing a way to connect the bare fibres to the spectrometers. The fiber output corresponding to in-coming REs (forward view) is connected to a low-OH bifurcated fiber (Thorlabs, BFY1000LS02 Bifurcated Fiber Bundle, ø1000 μ m Core, Low OH, SMA, 2 m) and thus to a set of two spectrometers, one operating in the visible (HR2000+, Ocean Optics, 300-860 ms) and the other in the infrared range (NIRQUEST256, Ocean Optics, 900-2500 ms) to permit the simultaneous detection of visible and infrared spectra of the collected synchrotron emission. The second fiber output, collecting the signal from out-going REs (backward view), is connected to a single spectrometer operating in the visible range (HR2000+, Ocean Optics, 300-860 ms).

B. Software architecture

The REIS system is supervised and managed by a dedicated LabVIEW program collecting data every 20 ms (configurable down to 10 ms) simultaneously from the three spectrometers and every 40 ms from the camera. The acquisition system is synchronized with the main common gate of the tokamak. Trigger time phasing for acquisition in external hardware triggering is represented in Figure 4. In case the collected signal is too low it is possible to increase the integration time.

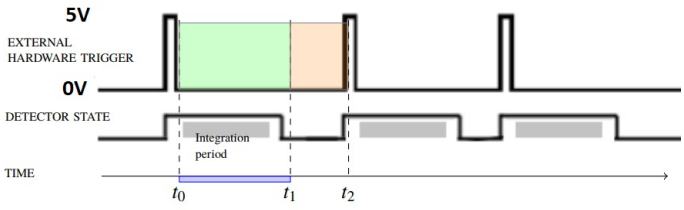

FIG. 4. Trigger timing phases. At first the system clean the memory then starts the integration for a fixed period of time (green box). Once the integration in over transfers the data to the host machine and waits for the next trigger (orange box), where t_0 is the acquisition time, t_1 is the integration time and t_2 data transfer time, corresponding to $t_0 = 0$ ms, $t_1 = 15$ ms and $t_2 = 20$ ms, respectively, in FTU.

The three spectrometers are synchronized by an NC

PCI-6602 (8-Channel Counter/Timer with Digital I/O) board that generates a preset number of pulses at a given frequency. Image acquisition is performed by an NI PCI-1411 card supporting analog format. The data acquisition system runs on a dedicated PC using LabVIEW for easy integration in different medium sized-tokamaks. The acquisition logic is based on a state machine pattern which is one of the fundamental architectures used in LabVIEW to implement complex decision-making algorithms represented by state diagrams, Figure 5. In the diagram, the states describe the actions that are performed when the control process is in that state, whereas the transitions (arrows) describe when and how the process can move from one state to another.

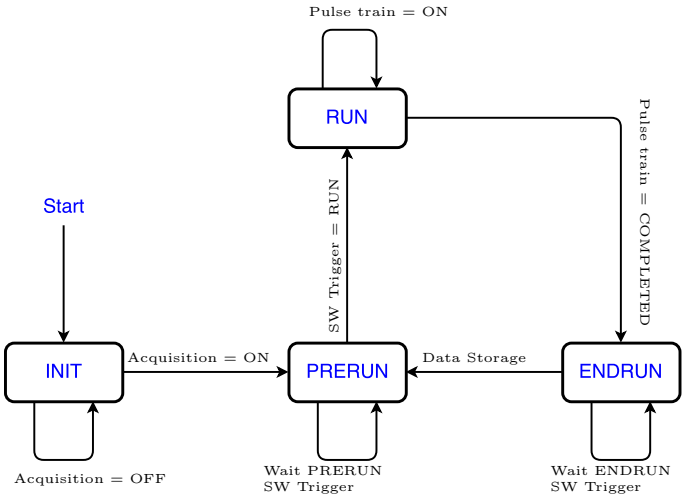

FIG. 5. REIS State Diagram

The REIS state diagram is composed of the following status:

1. INIT: this state is for the initialization, monitoring and control of hardware/software such as device type, integration time and number of acquisitions in accord with pulse train generator used for the control of the NC PCI-6602 board.

2. PRERUN: in this state the REIS system awaits for the software trigger, typically starting 30 s before the beginning of the pulse (referred to as 'zero plasma'). The software trigger is related to the state of a specific tokamak device, e.g, on FTU such state is retrieved by querying a specific database every 2 s. In the software trigger state it is also possible to retrieve the current pulse number. When the software trigger is high then the state machine moves into the RUN state.

3. RUN: in this state the REIS system is awaiting for the tokamak common gate to begin data acquisition. When the common gate is high then the system starts the acquisition of spectra and images. During the acquisition data is temporarily locally stored to be then saved on the REIS PC file system. Data acquisition is synchronized with the pulse train generated by a dedicated hardware installed of the REIS PC. When the pulse train is completed and no errors occur then the state machine moves into the ENDRUN state. The tokamak common gate is specific to the device on which the REIS is installed and must be taken into account during data processing, e.g, on FTU it starts at 50 ms before zero plasma.

4. ENDRUN: this state is dedicated to data storage on the REIS PC file system. Then the system moves back to the PRERUN state for a new acquisition.

In summary, the technical details of the REIS diagnostic are:

- **Spectrometers**
  VIS: 350-850 nm, CCD Line Array 2028 pixels (Ocean optics HR2000+)
  NIR: 900-2500 nm, CCD Line Array 256 pixels (Ocean optics NirQuest256)

- **Data Sampling**
  20 ms (integration time 15 ms + 5 ms for processing and data transfer).

- **Video Camera**
  CCD sensor imaging at 25 fps. Highly integrable system.

- **Portability**
  Designed to be installed easily on different tokamaks.

- **Automated data acquisition**
  Operated by dedicated LabVIEW program (synchronised via external time trigger).

C. Calibration

The REIS system was radiometrically relatively calibrated using two light sources: a medium-power tungsten Halogen Lamp (Osram eco 64702, 400 W,), referred to as WHL, and a low-power halogen calibrated source (Ocean Optics HL-3 Plus Cal Ext lamp, 45 W,), referred to as HL-3. Since the power and spectral range of the HL-3 lamp were insufficient for the calibration of both visible and infrared spectrometers, the calibration procedure was split into two steps.

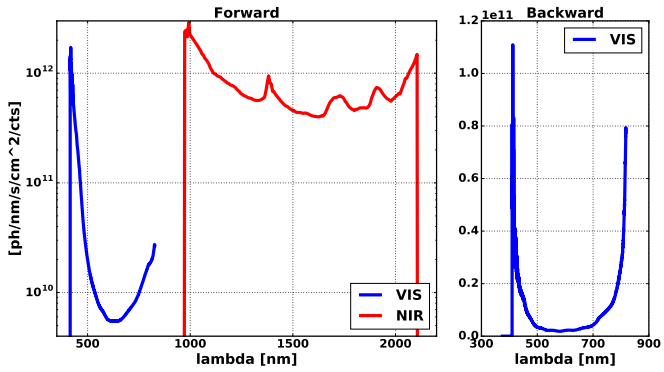

FIG. 6. Relative calibration curves.

In the first step HL-3 was used to calibrate the spectrometers in the visible range. Then WHL was used to extend the calibration into the near infrared range. The resulting relative calibration curves are presented in Figure 6 for the visible forward view (left column) and backward view (right column) spectrometers. In general a clear distinction can be observed between the spectra obtained from backward and forward view, as shown in Figure 7, demonstrating that the detected radiation from the forward view is indeed synchrotron emission from in-flight REs and that the effect of wall reflections is negligible.

III. EXPERIMENTAL RESULTS AND DISCUSSION

Experimental results were collected in FTU (major radius R=0.935 m, minor radius a=0.3 m, toroidal magnetic field B_{tor}=2-8 T), in different scenarios and operating conditions, including RE generation and suppression,[6] during the 2015, 2016 and 2017 experimental campaigns. As a representative case, data and corresponding analysis are discussed here in detail for pulse #41899 (B_t=5.5 T, $I_p = 0.35$ MA) from a 'RE generation and suppression' scenario, Figure 9. Synchrotron emission spectra (Figure 8) and RE beam images (Figure 10) from the REIS are also presented. The RE energy was estimated using equation 1, assuming mono-energetic distribution and constant pitch angle, for each experimental spectrum of Figure 8. The measured spectra used in the energy estimation procedure are calibrated, filtered using a Savitzky-Golay filter and finally cleaned from the emission lines from plasma impurities. Moreover, only data from spectral regions in which the uncertainty in the calibration is low have been kept for further analysis (namely 500-830 nm and 1480-2000 nm). In this procedure the best-fit total momentum p parameter is determined. The resulting fitted spectra (black dashed line) using this procedure are presented in Figure 8 at different times during the pulse. Before 240 ms and after 460 ms it was not possible to apply the analysis procedure to estimate the energy from the the spectrum because the signal to noise ratio was too low, as shown is Figure 8 (black and blue spectra). The time traces of plasma current I_p, loop voltage V_{loop}, electron density, neutron and gamma signals as well as the RE energy estimation (the latter limited to the time range 240 ms - 460 ms) are presented in Figure 9. REs are generated in the current ramp-up phase, as demonstrated by the difference between the time traces of NE213 scintillator (sensitive to gamma and neutrons) and BF_3 proportional counter (sensitive to neutrons only). A deuterium pellet was injected at t=0.152 s (red spike in Figure 9) and just after the onset of the RE plateau, at t=0.260 s, a molybdenum impurity was injected via laser blow-off (orange spike in Figure 9). Two more deuterium pellets (at t=0.479 s and t=0.548 s) increase the density of the plasma and a substantial suppression of the RE beam was finally achieved (t>0.5 s) as demonstrated by the neutron and gamma signals. From the RE beam energy estimation using the procedure described above, it was found that during the RE plateau the RE energy decreases gradually before a sudden peak occurring at 0.380 ms, corresponding to a loop voltage spike.

IV. CONCLUSIONS

The REIS is a new portable diagnostic developed to study in-flight REs. It was designed to be portable for use in present medium sized-tokamaks. The main features of the REIS as well as the calibration procedure have been described. An update of the REIS system is planned in 2018 to extend the wavelength range to 5000 nm for better coverage of the RE synchrotron emission spectrum, thus enabling (in some cases) the detection of the emission peak and in general improving the data interpretation capability.

ACKNOWLEDGMENTS

This work was carried out within the framework of the EUROfusion Consortium (project MST2-15: Runaway Electron Imaging) and received funding from the Euratom research and training programme 2014-2018 under grant agreement No 633053. The views and opinions expressed herein do not necessarily reflect those of the European Commission. The authors would like to thank M. Turnyanskiy, responsible officer for this EUROfusion project, for his continuous support and encouragement throughout this work. Finally, the authors wish to acknowledge Artur Perek (from DIFFER, Eindhoven, The Netherlands) for his help in performing the calibration of the REIS system.

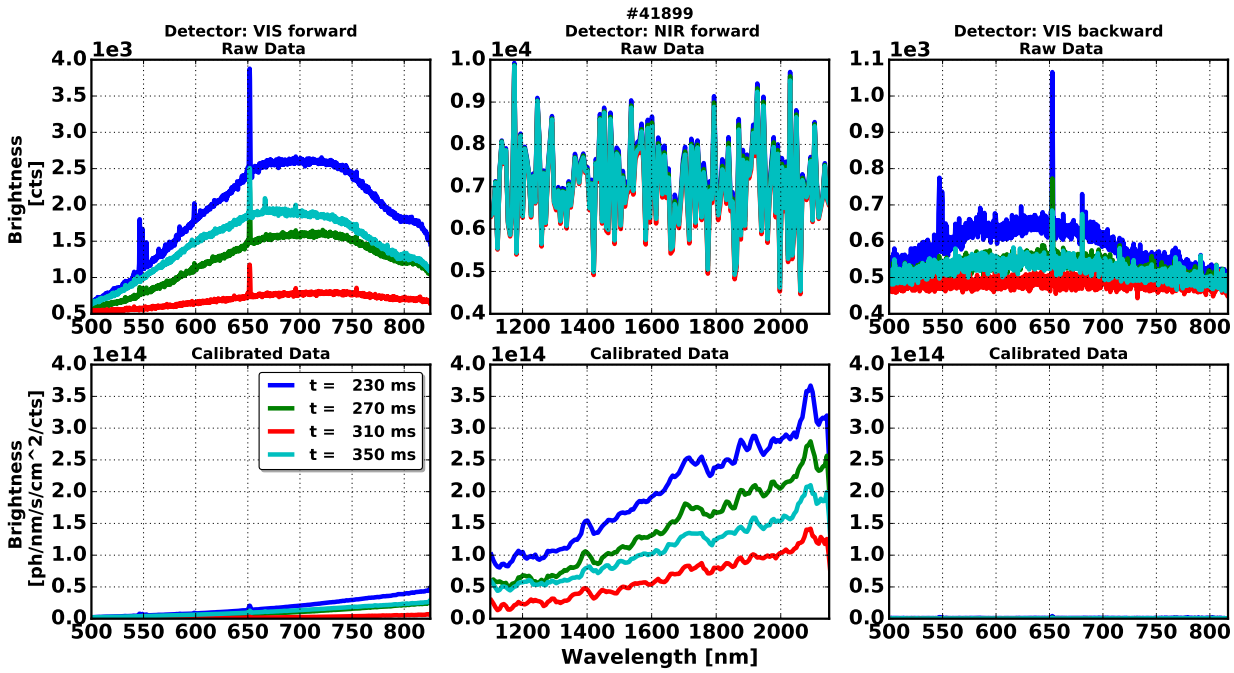

FIG. 7. Synchrotron emission radiation spectra in several time slices, discharge #41899, from forward (left and middle panels, for the visible and infrared parts of the spectrum, respectively) and backward (right panels) views. The raw count data, expressed as counts per second (cts), are in the top panels, the corresponding relative calibrated spectra in the lowers panels.

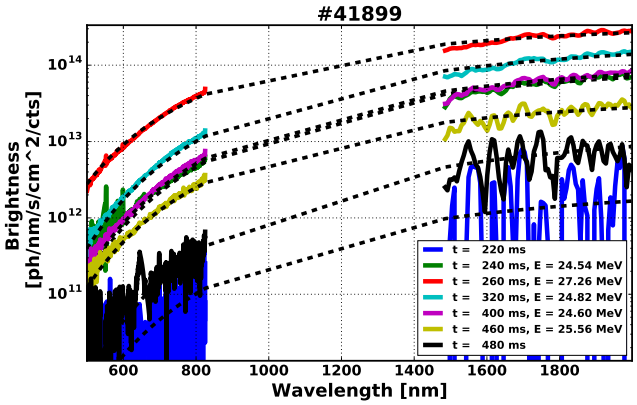

FIG. 8. Measured (solid curves) synchrotron radiation spectra and (dashed) fitted spectra calculated for a monoenergetic distribution and $\theta = 0.1$. Discharge #41899.

REFERENCES

[1]B. Esposito, L. Boncagni, P. Buratti, D. Carnevale, F. Causa, M. Gospodarczyk, J. Martin-Solis, Z. Popovic, M. Agostini, G. Apruzzese, W. Bin, C. Cianfarani, R. D. Angelis, G. Granucci, A. Grosso, G. Maddaluno, D. Marocco, V. Piergotti, A. Pensa, S. Podda, G. Pucella, G. Ramogida, G. Rocchi, M. Riva, A. Sibio, C. Sozzi, B. Tilia, O. Tudisco, M. Valisa, and F. Team, "Runaway electron generation and control," Plasma Physics and Controlled Fusion **59**, 014044 (2017).

[2]D. Carnevale, B. Esposito, M. Gospodarczyk, Z. Popovic, *et al.*, "Analysis of runaway beam suppression experiments in FTU," in *Preprint EUROFUSION WPMST2-CP(16) 15186, paper EX/P8-22 2016 IAEA Fusion Energy Conference* (2016).

[3]G. Pucella, E. Alessi, L. Amicucci, B. Angelini, M. Apicella, G. Apruzzese, G. Artaserse, F. Belli, W. Bin, L. Boncagni, *et al.*, "Overview of the FTU results," Nuclear Fusion **57**, 102004 (2017).

[4]J. Yu, E. Hollmann, N. Commaux, N. Eidietis, D. Humphreys, A. James, T. C. Jernigan, and R. Moyer, "Visible imaging and spectroscopy of disruption runaway electrons in diii-d," Physics of Plasmas **20**, 042113 (2013).

[5]A. Stahl, O. Embrus, G. Papp, M. Landreman, and T. Fülöp, "Kinetic modelling of runaway electrons in dynamic scenarios," Nuclear Fusion **56** (2016), 10.1088/0029-5515/56/11/112009.

[6]Z. Popovic, B. Esposito, J. Martín-Solís, W. Bin, P. Buratti, D. Carnevale, F. Causa, M. Gospodarczyk, D. Marocco, G. Ramogida, *et al.*, "On the measurement of the threshold electric field for runaway electron generation in the frascati tokamak upgrade," Physics of Plasmas **23**, 122501 (2016).

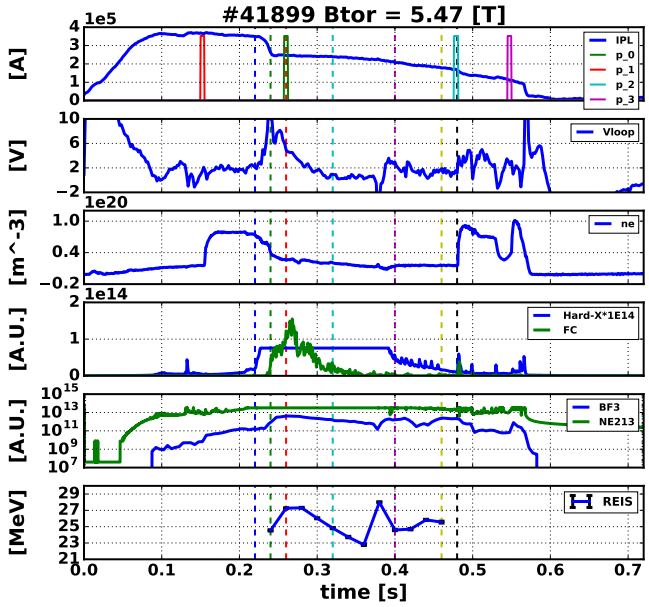

FIG. 9. Discharge #41899. (top) Time traces of the plasma current I_p, (second) loop voltage V_{loop}, (third) evolution of HXR monitor and fission chamber FC, (fourth plot) NE213 scintillator (green line) and neutrons from BF_3 (blue line) and (bottom) evolution of the energy fit parameter obtained from the REIS spectra between 240 ms and 480 ms.

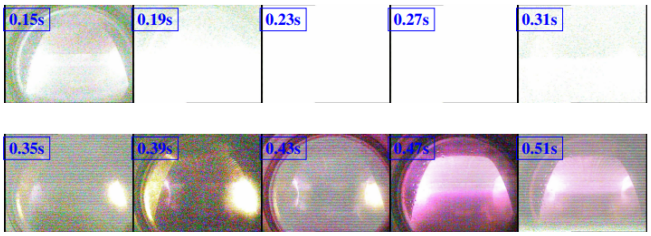

FIG. 10. Images of the synchrotron radiation captured by the REIS camera (installed on upper port 6) every 40 ms. Discharge #41899.